29 May 1998

ELSEVIER

Chemical Physics Letters 299 (1998) 727–733

CHEMICAL PHYSICS LETTERS

On self-limitation of UV photolysis in rare-gas solids and some of its consequences for matrix studies

Leonid Khriachtchev *, Mika Pettersson, Markku Räsänen

Laboratory of Physical Chemistry, University of Helsinki, P.O. Box 55, FIN-00014 Helsinki, Finland

Received 19 January 1998; in final form 5 March 1998

Abstract

UV photolysis of small molecules embedded in rare-gas matrices is examined. We demonstrate that photolysis can be self-limited when products absorb the photolysing radiation. As a result of the rising absorption, in-situ detected luminescence of the photolysis product saturates faster than its concentration. In particular, the present study supports the conclusion that 193 nm photolysis of hydrogen-containing species in Xe matrices produces hydrogen atoms in amounts comparable with the other dissociating part of the precursor. Also, we show that 193 nm radiation activates mobility of hydrogen atoms in annealing, accelerating photochemical processes related to hydrogen mobility.

1. Introduction

Matrix isolation is considered as a productive method for spectroscopic studies of atoms and molecules and their interactions including photochemical interconversion ([1], for a more recent review see Ref. [2]). Species under study are often unstable or difficult to deposit into a matrix directly and in this case they can be stabilized in a rare-gas host by photolyzing a suitable precursor.

In a number of matrix-isolation studies, UV photolysis of hydrogen-containing dopants is used [3–6]. After photoformation of atomic hydrogen in the parent cage, its cage exit and stabilization in the rare-gas host is quite probable at low temperature. Annealing to a certain temperature mobilizes the hydrogen atoms in the host, and they can reach other species to react. As an example, this approach was employed to generate a novel family of rare-gas containing molecules, such as HXeH, HXeBr, HXeI, HXeCl and HKrCl [7,8]. Recently, additional novel molecules HKrCN, HXeCN, HXeNC and HXeSH have been observed [9,10].

In solid xenon, atomic hydrogen forms a pseudomolecule Xe_nH (so-called caged hydrogen) [6,11–15]. The caged hydrogen is known to absorb photons in the 6.2–6.4 eV energy region, which brings it to the excited charge transfer states. These excited states decay radiatively and the emission can be observed at around 255 nm with a lifetime of about 40 ns.

This 255 nm emission of Xe_nH was used to follow the kinetics of atomic hydrogen concentration in 193 nm photolysis of HBr [16]. It was shown that the luminescence saturates much faster than the photolysis does and some loss mechanisms for atomic hydrogen were discussed. It was concluded that the

* Corresponding author. E-mail: khriacht@rock.helsinki.fi

0009-2614/98/$19.00
PII: S0009-2614(98)00295-4

maximum concentration of hydrogen atoms created during photolysis is more than an order of magnitude less than the maximum concentration of Br atoms [17].

However, our recent data on the formation and IR-induced decomposition of HXeI molecules employing HI photolysis proposes a much higher relative concentration of hydrogen atoms [18]. Indeed, up to 50% of the iodine atoms formed during photolysis were shown to participate in the formation of HXeI molecules in annealing. By taking into account the simultaneous diffusion-controlled formation of HXeH molecules, one can expect a large part of the hydrogen atoms to stabilize in solid xenon. This estimate was also quantitatively confirmed in the studies on formation of HXeNC/HXeCN molecules [9].

In this Letter, we explain the remarkable disagreement between the luminescence and infrared-absorption estimates on the concentration of hydrogen atoms in Xe matrices by employing the approach of optically thick matrices. This research was motivated by the importance of hydrogen atoms in low-temperature photochemistry and by the wide practical use of UV photolysis of hydrogen-containing species and luminescence probing. We have chosen HCN as a precursor for this study because of reliable IR detection of the precursor and CN radicals formed in the photolysis. Also, it is useful for our study that HCN is a quite weak absorber of 193 nm radiation [19].

2. Qualitative considerations and computational results

The known behavior of Xe_nH luminescence reported by LaBrake and Weitz [16] is the starting point for our consideration. In fact, under in-situ 193 nm photolysis, the emission reaches the saturation level when only a small portion of a hydrogen-containing precursor is photolyzed. Further photolysis results only in slow depletion of the steady-state emission. This experimental picture could be explained by employing extensive loss processes for hydrogen atoms. However, the studies of 193 nm photolysis of HI and HCN in Xe matrices propose a rather large proportion of hydrogen atoms [9,18] and here on we try to reconcile these two experiments.

In order to describe the luminescence kinetics, we consider the modifications of optical properties of the sample during the photolysis. It was shown by Fajardo and Apkarian that rare-gas matrices can often not be regarded as optically thin [20,21]. This makes it necessary to account for the depletion of the excitation field during its penetration into the matrix layer, and, in quantitative kinetic studies, the rate equations should be integrated over both time and depth. If the matrix contains a sufficient amount of a precursor, hydrogen atoms formed in the photolysis can provide strong absorption of the photolysis radiation and this decreases the photolysis efficiency for the deeper parts of the sample. Also, the excitation of hydrogen atoms becomes less efficient in the inner parts of the sample, which reduces the detected emission from that area. In other words, the luminescence method detects essentially the surface layer when the matrix contains a large number of hydrogen atoms. The estimations show that a 100 μm thick matrix with precursor/Xe = 1:2000 and an area of 1 cm^2 contains $\sim 2\times10^{17}$ precursor molecules. One 10 mJ pulse of 193 nm radiation consists of $\sim 10^{16}$ photons. This means that such a matrix can absorb totally the radiation after longer photolysis.

The qualitative picture can be put onto a quantitative level, similar to considerations by Fajardo and Apkarian [20,21]. We consider a matrix layer being photolyzed from one side. The photolysis efficiency is assumed to be proportional to $k_1 I(x,t)$ where $I(x,t)$ is the laser intensity in relative units at a given coordinate and time and k_1 is the photolysis time constant for $I(x,t)=1$. The relative concentration of hydrogen atoms $n_H(x,t)$, establishes the absorption coefficient $k_2 n_H(x,t)$, the factor k_2 depending on the transition oscillator strength. The luminescence signal from hydrogen atoms can be written as

$$S(t) = Ak_2 \int_0^L I(x,t)\, n_H(x,t)\, dx \qquad (1)$$

where A describes the efficiency of luminescence detection and L is the thickness of the matrix layer. In this simple model, the precursor absorption is neglected.

Fig. 1 presents the precursor concentration and the photolysis laser intensity as a function of the penetration depth for two different photolysis times.

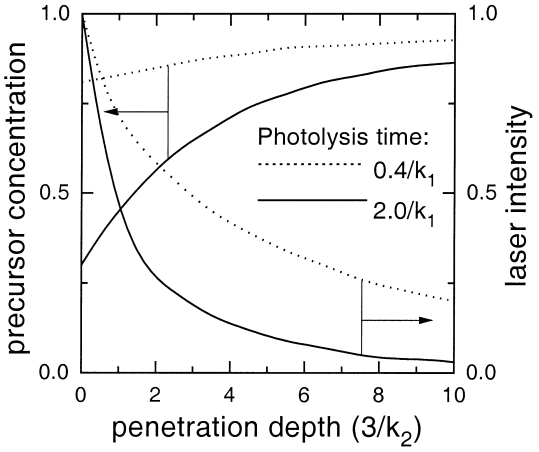

Fig. 1. The precursor concentration and the laser intensity as a function of penetration depth into matrix bulk calculated for two photolysis times. The arrows show the axes, to which the curves refer.

In the beginning of the photolysis, both the precursor concentration and the laser intensity are set equal to 1. During the photolysis, the medium becomes more absorbing. This absorption leads to a decrease of the laser intensity with depth. As a result, the photolysis is more efficient near the surface, compared with deeper in the bulk, where it slows down with time. Thus, the progress of the photolysis reduces its efficiency, i.e. self-limitation of the process takes place.

Fig. 2 compares the kinetics of the product concentration and the corresponding luminescence for two thicknesses of the sample with the same precursor concentration. For the thinner sample, the difference between the two curves is not dramatic, about 20%. For the thicker sample, the curves differ greatly, in particular, the luminescence starts saturating when only about 30% of the precursor is photolyzed. Similarly, the concentration and luminescence kinetic curves become closer to each other for more diluted matrices and the difference increases with the initial precursor concentration.

Our calculations explain qualitatively the difference between the kinetics of atomic hydrogen concentration and the corresponding luminescence. However, it is clear that the results give only qualitative trends without accurate estimates and we can mention at least two important factors, which make more quantitative consideration difficult. The first factor is the influence of Rayleigh scattering. This non-coherent effect changes the direction of the light wave propagation due to optical inhomogenity of the medium. Essentially, the intensity distribution after scattering is written as

$$I_\theta \sim (1 + \cos^2\theta)/\lambda^4 \qquad (2)$$

where θ is the angle of scattering and λ is the radiation wavelength (see for instance Ref. [22]). It is important to note that the cross-section of Rayleigh scattering increases with radiation frequency. While a sample does not scatter much in IR absorption measurements, it can be significantly scattering at the photolysis wavelength. From the viewpoint of the effect under discussion, Rayleigh scattering can enhance the effective absorption of the sample because it increases the pathlength of the radiation in the sample bulk. This is illustrated by Fig. 3 where we compare the spatial distributions of photolysis efficiency with and without scattering. The influence of scattering was estimated by a simple model of one-dimensional scattering (forward and back) with absorption happening after twelve scatterings of a photon. It is evident from Fig. 3 that Rayleigh scattering limits strongly the penetration of radiation into the bulk and enhances the radiation intensity in the surface layer. In reality, three-dimensional scattering in inhomogeneous matrix morphology can produce

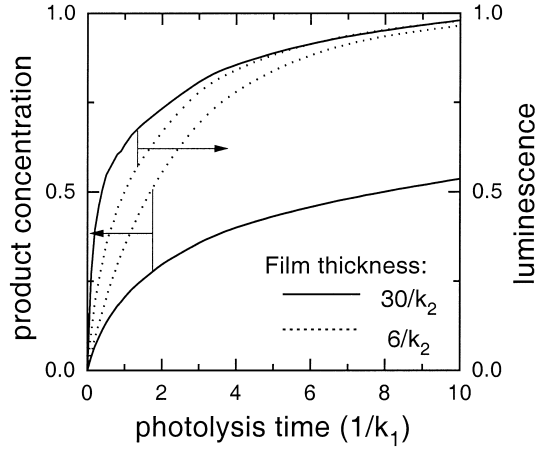

Fig. 2. The product concentration and the product luminescence as a function of photolysis time calculated for two matrix thicknesses. The arrows show the axes to which the curves refer.

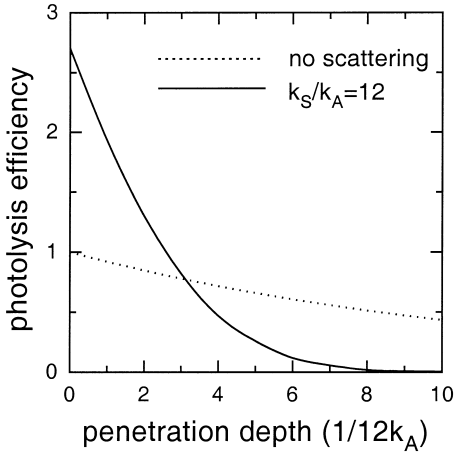

Fig. 3. The photolysis efficiency as a function of penetration depth into matrix bulk calculated for two cases, without scattering ($k_S = 0$) and with scattering ($k_S / k_A = 12$). The absorption (k_A) was assumed to be constant along the coordinate and one dimensional scattering was treated.

complicated modification of the laser radiation distribution in the sample bulk. Secondly, some additional absorbers to some extent can influence the result. For example, the absorption of the precursor was neglected in our computations because of its weakness [19]. Also, some modification of luminescence kinetics can arise from minor absorption of luminescence photons by matrix impurities (molecular oxygen, as an example) and water impurities can contribute to atomic hydrogen concentration.

3. Experimental apparatus and results

The experiments were performed with solid-state xenon matrices doped with HCN in various proportions (typically 1:2000) prepared by a standard manometric technique with synthesized HCN [1] and xenon (> 99.99%, Aga). The gas mixture was deposited onto a CsI substrate at 7.5 K in a closed cycle helium cryostat (HC-2, APD). The temperature was measured with a silicon diode (accuracy 0.5 K) and a resistive heater provided higher temperatures.

The HCN samples were photolyzed by an excimer laser (ELI 76, Estonian Academy of Science) at 193 nm, with pulse energies up to 20 mJ and a pulse duration of ~ 10 ns. The spectra were recorded with an FT-IR spectrometer (Nicolet 60SX) and with a single UV–VIS monochromator (Spex 270M) equipped with a gated ICCD camera (Princeton Instruments). The concentrations of HCN and CN were measured as proportional to the IR absorptions at 718 [24] and 2040 cm^{-1} [9,25], respectively.

A typical UV emission generated by 193 nm photolysis of the samples is shown in Fig. 4a and it agrees well with the literature data on Xe_nH emission. It should be noted that this 255 nm emission undergoes some shape changes during photolysis. The shape can be stabilized by annealing after photolysis (to 40 K), with Fig. 4a showing emission of such an annealed sample. The stabilization upon annealing suggests a site origin of the effect and similar trends were noticed, for instance, by Zoval and Apkarian for sulfur atoms in argon and krypton matrices [5]. This interesting phenomenon of the emission modification is under study in our laboratory.

Under 193 nm photolysis of HCN in Xe matrices, decomposition of HCN correlates reasonably well with the formation of CN radicals although some formation of HNC isomers takes place as indicated by the absorptions at 3577, 2021 and 477 cm^{-1} [9,26]. [2] The 255 nm emission saturates faster than decomposition of the precursor happens, in agreement with the observation by LaBrake and Weitz [16]. This saturated value decreases slowly in longer photolysis and sometimes some persistent proportion of the precursor is observed.

In order to test the hypothesis described above, we followed the time-dependence of the 255 nm emission. Just after saturation of the emission, we measured a level of HCN decomposition. The experiment was run for three samples with the same HCN/Xe ratio (1:2000) and different thicknesses

[1] HCN was synthesized from H_2SO_4 and KCN [23], dried with phosphorus pentoxide and purified by vacuum distillation.

[2] In Ref. [26], the absorptions of HNC were measured in Ar matrixes and the results correlate well with our measurements in solid xenon. To our knowledge, there is no literature data about HNC IR absorptions in Xe matrixes.

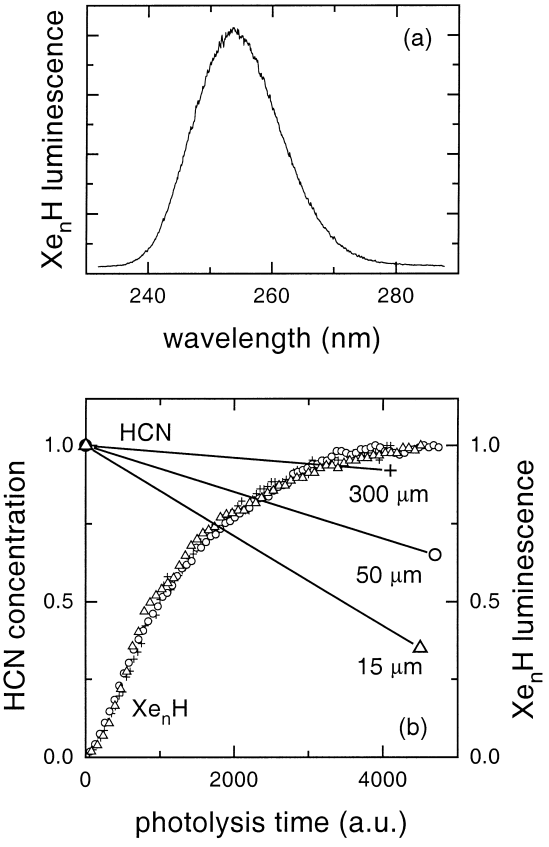

Fig. 4. 193 nm photolysis of HCN in solid xenon at 7.5 K. (a) The in-situ excited Xe_nH emission spectrum. (b) Comparison of data for HCN concentration measured by IR absorption with luminescence kinetics measured for three matrix thicknesses 300 (crosses), 50 (circles) and 15 μm (triangles). The radiation with ~3 mJ/pulse/cm^2 was used for photolysis. The luminescence data were scaled to approximately coincide to each other. The lines are used for guiding the eye.

300, 50 and 15 μm. The thickness of the thinner matrix was measured from interference patterns in the IR absorption spectra and the ratios were confirmed by comparing the HCN IR absorptions, which were found to correlate with the deposition times.

The comparison of decomposition efficiencies for the three samples is presented in Fig. 4b, the time-axis being scaled to overlap the luminescence dependencies. As the most essential result, a strong difference in the precursor decomposition efficiency was observed for the three samples. For the 300, 50 and 15 μm thick samples, respectively, decomposition of about 10%, 30% and 65% corresponds to the same saturation level of atomic hydrogen emission (~90% of the maximum). This result is in perfect agreement with the previous discussions.

Also, we carried out the same measurement using a ten times more diluted sample (HCN/Xe = 1:20000) with matrix thickness of 300 μm. The dilution was found to slow down saturation of the 255 nm emission relative to the decomposition of HCN, again in agreement with our calculations. For this last sample, the saturation of the emission (~90% of the maximum) corresponds to about 30% decomposed HCN, which is three times more than that proportion for the ten times more concentrated sample of the same thickness.

In a final experiment, we studied thermal bleaching of the 255 nm luminescence and the influence of irradiation on this process. A sample (HCN/Xe = 1:20000) was first properly photolyzed at 7.5 K. Then, we increased the temperature to 50 K and detected the luminescence excited by weak probing radiation. The luminescence was measured every 10 min for 10 s with the pulse energy density < 0.1 mJ/cm^2 at a 2 Hz repetition rate and such probing irradiation was found not to influence the bleaching process much. This essentially temperature-induced bleaching is shown in the first stage of Fig. 5 (0–80

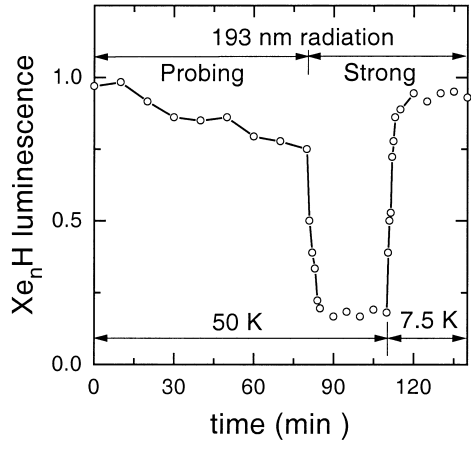

Fig. 5. Kinetics of Xe_nH emission signal in different experimental conditions. The strong 193 nm radiation has a pulse energy density of about 10 mJ/cm^2 at 2 Hz. The probing radiation used at the first stage is weaker by a factor of 100 and the period of a measurement was limited to 10 s. The luminescence signals under strong and probing radiation are normalized to each other at the point of switching the strong radiation on. The cooling period (from 50 to 7.5 K) is excluded.

min). Then, we applied strong 193 nm radiation to the sample (~ 10 mJ/pulse/cm^2, 2 Hz). A fast decrease of the 255 nm emission was observed as shown in the second stage of Fig. 5 (80–110 min), the luminescence signal being normalized to that excited by the weak probing radiation. The emission signal saturates at some level ($\sim 20\%$ of a starting level) and does not change more under longer irradiation. When the temperature of the sample was lowered to 7.5 K (the cooling period is not shown in the picture), the strong irradiation returned the luminescence signal to rather close to the starting level. Such cycles under the strong irradiation (photo-induced bleaching at 50 K and photolysis at 7.5 K) can be repeated without an essential decrease of the steady-state emission.

4. Discussion

The experiments described above distinguish two possible origins of the different time dependencies for Xe_nH luminescence and HCN decomposition: absorption of the photolysis radiation and possible chemical losses. In the model of self-limited photolysis, decomposition of the precursor and product luminescence depend on the sample thickness in different ways. Namely, decomposition of the precursor takes longer and the luminescence saturates faster for thicker samples, i.e. their kinetics have an opposite thickness dependence. Of course, the loss reactions discussed in Refs. [16,17] are independent of film thickness. Thus, the difference in kinetics of photolysis efficiency and luminescence of photolysis products arises essentially from the increasing absorption of the medium at the photolysis wavelength. [3]

The effect under discussion occurs when the photolysis products absorb the photolyzing radiation and the photolyzed front layer covers the bulk preventing further photolysis. From this point of view, the limitation of photolysis efficiency is essentially self-limitation. The self-limitation of the photolysis explains the persistent part of the precursor, which is often observed in practice. In the framework of the present study, this limitation is most probable in matrices of poor optical quality providing efficient scattering. The effect under discussion takes place when hydrogen atoms in Xe matrices are generated by 193 nm photolysis of HCl, HBr, HCN, H_2S, etc. As a further example, we can mention photolysis of hydrogen peroxide at wavelengths resonant with OH radicals.

Also, the absorption of photolysis radiation by the products influences the in-situ detected luminescence of the products. In particular, the luminescence does not follow the concentration of the products but saturates faster than the concentration does. This applies especially to scattering samples. In photolysis experiments with Xe matrices, we noticed often some increase of scattering, which was visible in the IR spectra. According to the present discussion, the possible increase of scattering during photolysis reduces the luminescence signal when the concentration is constant. This process may be responsible for the experimentally observed decrease of the 255 nm luminescence during long photolysis.

The analysis of the present results together with our recent data on IR decomposition of HXeI [18] supports the conclusion that the major part of the dissociated hydrogen atoms is stabilized in the matrix. In annealing, most of the hydrogen atoms participate in the formation of such xenon-containing species as HXeH and HXeI, and only a minor part of them restores the precursor and forms H_2, for instance, in the reaction

$$H + HI \rightarrow H_2 + I. \quad (3)$$

More extensive discussions of this subject can be found elsewhere [18]. It should be noticed here that the hydrogen atoms arising from dissociation of water impurities are neglected. This approximation is justified because the impurity water concentration was estimated to be less than 1:20000. The strong dependence of the hydrogen luminescence on the HCN concentration supports this approximation at least for the matrices with HCN/Xe = 1:2000. In the framework of the present study, dissociation of water impurities slows down the photolysis and ac-

[3] We obtained more experimental evidence of this conclusion while studying 193 nm photolysis of HCN in Kr matrices. CN radicals in solid krypton were found to absorb the 193 nm radiation and the CN emission at ~ 790 nm was detected. Thus, we could measure both luminescence and IR absorption of the same product. Indeed, the CN luminescence saturated faster than CN concentration measured by IR absorption.

celerates the saturation of the luminescence and this process can influence particularly the kinetics measured in the more diluted (HCN/Xe = 1:20000) sample.

In luminescence kinetics studies, it is also quite important to account for the radiation-induced enhancement of the hydrogen mobility because the probing radiation can change the concentration influencing the estimates of the rate constants. Fig. 5 demonstrates the increase of atomic hydrogen mobility while irradiating the matrix at 50 K. This temperature (50 K) is known to mobilize hydrogen atoms in Xe matrices [6] and their thermal diffusion causes the slow decay of the luminescence without irradiation. The 193 nm irradiation gives some additional kinetic energy to individual hydrogen atoms in the process of Xe_nH decay, and the mobility of hydrogen atoms enhances dramatically, about by a factor of 10^2 in our experiments, thus dominating the thermal mobility at 50 K. On the other hand, Fig. 5 also proves the essential participation of the lattice in atomic hydrogen mobility. Indeed, when decreasing the temperature, we obtained stabilization of hydrogen atoms again in the network. Thus, it is not enough for an atom to have kinetic energy to travel from cage to cage but also the lattice should be activated. It seems to us that the observed behavior can be interpreted by using the known model of local lattice melting developed by Tarasova et al. [4].

5. Conclusions

In the present study, we have demonstrated that UV photolysis in solid-state matrices can be self-limited when the photolysis products absorb the photolysis radiation. Practically, this leads to slowing down the photolysis efficiency with time. The growth of the absorbers can lead to fast saturation of the in situ detected luminescence. As a result, the luminescence signal does not follow the product concentration accurately. The 193 nm photolysis of hydrogen-containing species in Xe matrices produces hydrogen atoms in amounts comparable with the other dissociating part of the precursor. In annealing, these parts recombine mainly into xenon-containing neutral species. Additionally, 193 nm radiation activates the mobility of the hydrogen atoms during annealing. This radiation-enhanced mobility accelerates photochemical processes involving hydrogen mobility.

References

[1] L.E. Andrews, M. Moskovits (Eds.), Chemistry and Physics of Matrix Isolated Species (Elsevier, Amsterdam, 1989).
[2] V.E. Bondybey, A.M. Smith, J. Agreiter, Chem. Rev. 96 (1996) 2113.
[3] H.M. Kunttu, J.A. Seetula, Chem. Phys. 189 (1994) 273.
[4] E.I. Tarasova, A.M. Ratner, V.M. Stepanenko, I.Ya. Fugol, M. Chergui, R. Schriever, N. Schwentner, J. Chem. Phys. 98 (1993) 7786.
[5] J. Zoval, V.A. Apkarian, J. Phys. Chem. 98 (1994) 7945.
[6] J. Eberlein, M. Creuzburg, J. Chem. Phys. 106 (1997) 2188, and references therein.
[7] M. Pettersson, J. Lundell, M. Räsänen, J. Chem. Phys. 102 (1995) 6423.
[8] M. Pettersson, J. Lundell, M. Räsänen, J. Chem. Phys. 103 (1995) 205.
[9] M. Pettersson, J. Lundell, L. Khriachtchev, M. Räsänen, J. Chem. Phys. (1998) in press.
[10] L. Khriachtchev, M. Pettersson, E. Isoniemi, M. Räsänen, J. Chem. Phys. 108 (1998) 5747.
[11] M. Creuzburg, F. Koch, F. Wittl, Chem. Phys. Lett. 156 (1989) 387.
[12] F. Wittle, M. Creuzburg, R. Schriever, J. Lumin. 48/49 (1991) 611.
[13] M. Kraas, P. Gürtler, Chem. Phys. Lett. 174 (1990) 396.
[14] M. Kraas, P. Gürtler, Chem. Phys. Lett. 183 (1991) 264.
[15] M. Creuzburg, F. Wittle, J. Mol. Struct. 222 (1990) 127.
[16] D. LaBrake, E. Weitz, Chem. Phys. Lett. 211 (1993) 430.
[17] D. LaBrake, E.T. Ryan, E. Weitz, J. Chem. Phys. 102 (1995) 4112.
[18] M. Pettersson, J. Nieminen, L. Khriachtchev, M. Räsänen, J. Chem. Phys. 107 (1997) 8423.
[19] H. Okabe, Photochemistry of Small Molecules, 1st edn. (Wiley, New York, 1978).
[20] M.E. Fajardo, V.A. Apkarian, J. Chem. Phys. 85 (1986) 5660.
[21] M.E. Fajardo, V.A. Apkarian, J. Chem. Phys. 89 (1988) 4102.
[22] P.W. Milloni, J.H. Eberly, Lasers (Wiley, New York, 1988).
[23] E. Knözinger, R. Wittenbeck, J. Chem. Phys. 80 (1984) 5979.
[24] A.D. Abbate, C.B. Moore, J. Chem. Phys. 82 (1985) 1255.
[25] G. Schallmoser, A. Thoma, B.E. Wurfel, V.E. Bondybey, Chem. Phys. Lett. 219 (1994) 101.
[26] D.E. Milligan, M.E. Jacox, J. Chem. Phys. 47 (1967) 278.